Invited Paper

Time-dependent studies of high-order harmonic generation

Kenneth J. Schafer, Jeffrey L. Krause and Kenneth C. Kulander

Physics Department, Lawrence Livermore National Laboratory
L-299, Livermore, CA 94550

and

Anne L'Huillier

Service de Physique des Atomes et des Surfaces, Center d'Etudes Nucléaires de Saclay
91191 Gif-sur-Yvette, France

ABSTRACT

Experimental results have demonstrated very high order harmonic generation in rare gases exposed to intense laser fields. We use time-dependent methods to calculate the single atom emission spectrum in a number of systems. These spectra show many of the same features seen experimentally, e.g. a broad plateau that depends in intensity and extent on the ionization potential. To explain the observed spectra, we fold these single atom results into a full solution of the propagation equations for the nonlinear medium. This leads to impressive agreement between theory and the experiment for xenon, both in the absolute number of photons observed as well as the intensity dependence of all harmonics through the 21st. The use of time-dependent methods also facilitates a comparison between photon and electron emission processes.

INTRODUCTION

Over the past few years, several experimental groups have demonstrated the production of high order optical harmonic generation from atoms subject to intense laser fields.[1,2] Up to the 53rd harmonic of the Nd:YAG (1064 nm) has been produced in neon[3] with intensities of ~ 10^{13} - 10^{14} W/cm^2, and wavelengths as short as 15 nm have been reported using a KrF (248 nm) pump laser.[2] These experiments have been performed with intense, short-pulsed lasers focused onto a high density gas jet. Recently the 97th harmonic of an 800 nm laser was observed in a gas cell filled with neon.[4] Observation of high order harmonic generaton requires proper phase matching conditions within the focal volume of the laser. The emitted harmonics are coherent and the macroscopic harmonic intensities are proportional to the square of the density of the radiating atoms.[5] The efficient conversion of long wavelength radiation to much shorter wavelengths has a wealth of possible applications which are only beginning to be explored. Their brightness is at least comparable to conventional synchrotron sources, raising the possibility of developing optical harmonic generation as a useful source of vacuum ultraviolet to possibly X-ray photons.[2]

Optical harmonic generation takes place in an intensity regime where traditional perturbation theory breaks down (intensities greater than 10^{11} W/cm^2 for 1064 nm, the fundamental of the Nd:YAG laser).[6] At these intensities, the assumption that the laser field causes only small perturbations of the field-free atomic states is no longer valid. Calculations of, for example, ionization rates via lowest-order perturbation theory or of harmonic generation using intensity-independent susceptibilities are completely inadequate.[6,7] We have therefore chosen to use explicit integration of the time-dependent Schrödinger equation (TDSE) to generate the electronic wave functions needed for the calculation of photon and electron emission rates. This allows us to treat the intra-atomic interactions on an equal footing with the laser-electron interactions, making no assumptions about the relative strengths of these forces. Our numerical method has the flexibility to treat a wide range of laser intensities, wavelengths and pulse shapes, as well as different atomic and molecular systems.

NUMERICAL METHOD

The approach we use is based on the knowledge that the wave function of an electron in a strong laser field is in general quite complicated. For example, an electron, after reaching the continuum, continues to oscillate in response to the field as it drifts away from the atom. For this reason, the traditional expansion of the wave function in field-free atomic states

0-8194-0679-1/92/$4.00

is very slowly convergent. Therefore, we have chosen to use a finite-difference representation of the wave function on a numerical grid. Numerical wave functions have the flexibility to represent the anticipated complicated behavior efficiently.

We have considered to date only the case of a linearly polarized, spatially homogeneous laser field. In this case, the system possesses cylindrical symmetry; the azimuthal quantum number of the electron (conventionally denoted by *m)* is conserved meaning the number of significant spatial dimensions is two. This greatly reduces the computational requirements. We have utilized grid representations with both cylindrical and spherical coordinate systems. The former is more convenient in the velocity gauge and the latter in the length gauge. All of the calculations that we will discuss were performed using spherical coordinates and in the length gauge. We will only briefly sketch the numerical methods that we have used. Further details can be found in a recent review.[8]

Consider the case of a one-electron atom (with $m=0$) in a laser field linearly polarized along the z axis ($m \neq 0$ is easily treated by the same formalism with only minor changes). We expand the electronic wave function in spherical harmonics,

$$\psi(r,\theta,\phi,t) = \sum_{\ell=0}^{L} \frac{\Phi_\ell(r,t)}{r} Y_\ell^o(\theta,\phi), \tag{1}$$

up to a maximum angular momentum L, chosen large enough to insure convergence. The Hamiltonian has two pieces, a field-free atomic term, H_A^ℓ, which is time-independent and diagonal in the ℓ quantum number, and an interaction term which is, in the dipole approximation,

$$H_I = -\varepsilon_o f(t) z \sin(\omega_o t). \tag{2}$$

This term couples angular momenta ℓ to $\ell \pm 1$, which corresponds to the absorption or emission of a single photon. $\mathcal{E}_O$ and ω_O are the peak amplitude and frequency of the laser field, and $f(t)$ defines the pulse envelope. The full TDSE for this system is, in atomic units ($e = m = \hbar = 1$),

$$i\frac{\partial}{\partial t}\psi(r,t) = \left\{H_A^\ell + H_I\right\}\psi(r,t), \tag{3}$$

We insert the expansion in Eq. (1) into Eq. (3) and discretize the resulting coupled equations along the radial direction. The time integration is achieved by propagating the initial state, ψ at $t=0$, forward in time with a Peaceman-Rachford propagator.[9] The time propagation is very efficient, allowing for the determination of about 1.2 million space-time points per CPU second on a Cray Y/MP.

For a hydrogenic ion H_A^ℓ is simply

$$H_A^\ell = -\frac{1}{2}\frac{d^2}{dr^2} + \frac{\ell(\ell+1)}{2r^2} - \frac{Z_n}{r}, \tag{4}$$

where Z_n is the nuclear charge. In this case the solution is exact to within numerical accuracy. For multielectron atoms the situation is, of course, more complicated. We have developed a linear approximation to the full multielectron equations called the single active electron model (SAE).[10] As the name implies, the SAE assumes that a multielectron atom ionizes sequentially, one electron after another. Our experience has been that this is a good approximation, implying that double excitations can be ignored for the intensities and wavelengths that we will consider in this paper. Within the SAE we calculate the time-dependent wave function for the active electron as it moves in response to the laser field in the time independent mean field of the remaining electrons in their ground state orbitals.

The mean field potential for the active electron is generated from a Hartree-Slater calculation[11] for either the ground state or an excited state, with different potentials for different orbital angular momenta ℓ. This amounts to replacing the term $-Z_n/r$ in Eq. (4) with a term

$$V(r) = \sum_{\ell=0}^{L} V_\ell(r). \tag{5}$$

For example, for the xenon 5p orbitals we obtain the $\ell = 1$ potential from a ground state calculation and the $\ell = 0$ and $\ell = 2$ potentials from $5p^5 6s$ and $5p^5 5d$ calculations, respectively. For $\ell > 2$ we use the $\ell = 2$ potential. In the Hartree-Slater calculations we vary the scaling parameter in the exchange-correlation potential to obtain an accurate ionization potential for the state. Also, the modification of the Hartree-Slater equations to incorporate the correct, long-range Coulomb attraction has necessarily been included. The effective potential is constructed by removing the nodes from the valence orbital of interest, following the prescription of Christiansen et al.[12] and Kahn et al.,[13] and then inverting the single particle Schrödinger equation for this pseudo-orbital to obtain $V_\ell(r)$. The prescription we have outlined here has been shown to work well for the rare gases that we have studied.[14]

HIGH ORDER OPTICAL HARMONIC GENERATION

The main features of experimental harmonic generation spectra are a rapid decline from the first to about the fifth harmonic, as one would expect from perturbation theory, followed by a "plateau" region, extending to high order across which the harmonic intensity drops by only about one order of magnitude, and then a rapid decline, referred to as a "cut-off", in the spectrum.[15] Underlying this structure is a broad background. In this section we first give a brief account of our calculations of single atom harmonic emission spectra. We then discuss how we relate these spectra to the experimental spectra. Although the two spectra share many superficial features, calculations of sufficient quality to provide predictions of absolute harmonic intensities require the solution of the full propagation equation for the harmonics in the nonlinear medium. This many body calculation has as its basic input the non-perturbative, single atom polarization which we first calculate.

The calculation of single atom spectra is straightforward within the time-dependent formalism. We need only calculate the time-dependent dipole moment induced in the atom by the laser.[16] For light linearly polarized along the z direction this is simply

$$d(t) = \langle \psi(t) | z | \psi(t) \rangle. \tag{6}$$

The single atom emission spectrum is proportional to the square of the Fourier transform of this dipole,

$$\sigma(\omega) \propto |d(\omega)|^2 = \left| \frac{1}{T} \int_0^T dt\, e^{-i\omega t} d(t) \right|^2. \tag{7}$$

We will refer to $|d(\omega)|^2$ as the single atom spectrum. Momentum conservation requires that photon absorption and emission can take place only when the electron is close to the nucleus. Therefore, we need not calculate $\psi(t)$ at distances where the electron is ionized and travelling away from the nucleus. We use a moderately sized (~100 a.u.) computational box with a smoothly-varying mask function near the outer radius to remove from the grid any portion of the wave function that has left the vicinity of the nucleus. Since electrons that travel this far from the nucleus cannot be recaptured, we assume that they are ionized and play no further role in photoemission.

A typical single atom spectrum, $|d(\omega)|^2$, is shown in Fig. 1. This spectrum is for the xenon $5p_0$ orbital at 1064 nm and an intensity of 2×10^{13} W/cm^2. We use a pulse envelope with a five optical cycle linear ramp and a constant intensity interval of 15 - 25 cycles. The Fourier transform is performed over five cycles late in the flat portion of the pulse to limit the effect of transients caused by the turn-on of the laser field. The spectrum is dominated by strong, narrow peaks at odd harmonics of the driving laser. As is well known, an isolated atom in a continuous wave laser field has inversion symmetry, so the even harmonics are forbidden.[5] There is also a broad background underlying the spectrum. The features discussed in connection with experimental spectra are all apparent in the single atom spectrum, i.e., a rapid initial decline, a plateau and then another precipitous decline.

Examination of several such spectra at differing intensities reveals a pattern which we have found in all of our calculations. As the intensity increases, the level of the plateau increases and broadens. In perturbation theory the strength of the qth harmonic scales as I^q, where I is the laser intensity. As perturbation theory begins to break down, the intensity

dependence becomes much weaker. Eventually, many different harmonics merge to form a plateau in which all of the harmonics have about the same intensity dependence. This intensity dependence is of much lower order than that predicted by perturbation theory. Close examination of the data shows that for xenon at 1064 nm, the plateau scales as about I^5. As the laser intensity increases, the individual harmonics exhibit numerous resonances and structures, with the overall trend being a transition from an initial high order dependence on the laser intensity to an approximately I^5 behavior above 2.0 10^{13} W/cm^2. All of the harmonics show this general pattern as a function of intensity.

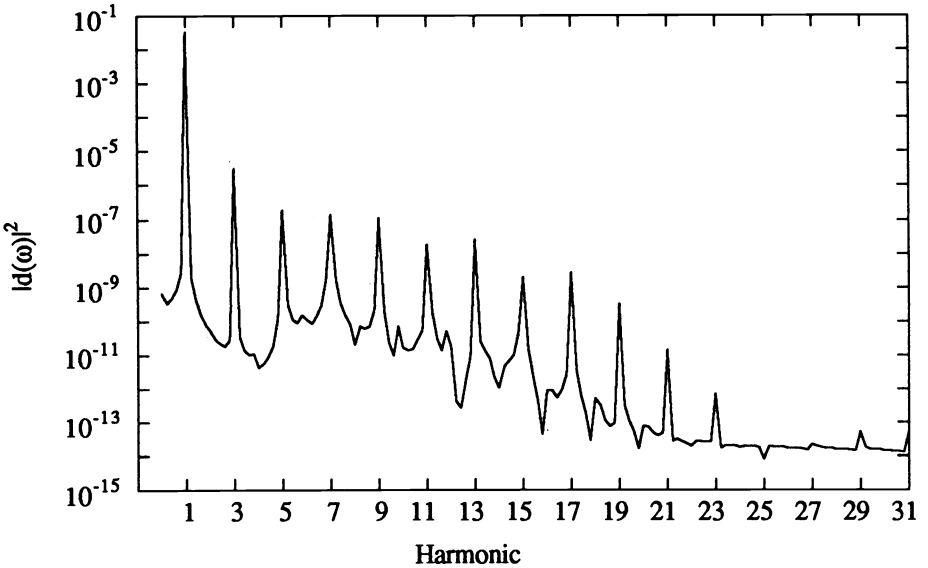

Fig. 1. Optical harmonic generation single atom spectrum ($|d(\omega)|^2$) for xenon, 1064 nm laser at 2.0 10^{13} W/cm^2.

Experimentally observed harmonic generation is a coherent process and therefore a many atom phenomena. The process of obtaining predictions for observed spectra from the single atom calculations described above proceeds in two steps.[15,17] First, spectra emitted by a single atom are calculated for a range of laser intensities to model the spatial distribution of intensities present in the focus of the laser. These single atom spectra consist of the magnitude of $d(\omega)$ and its phase relative to the driving field. For coherent emission to be possible, the harmonic must carry a constant phase relative to the driving field, or contributions from many different atoms will add destructively. We find that only the odd harmonics of the driving field carry a constant phase. At all other frequencies the phase is a rapidly varying function from cycle to cycle. This leads to the observation that the background found in our single atom spectra (and in all other calculations of single atom and model atom spectra to our knowledge) cannot be identified with the experimentally observed background. Given the high gas density used in the experiments (10^{17} atoms/cm^3) incoherent processes which scale as the density such as the single atom background, would not be observable on the same scale as the harmonic radiation which is proportional to the square of the density. The experimental background, which is clearly observable, arises in part from sources not included in our calculation. For example, the experimental background contains many closely spaced fluorescence lines due to recombination, which occurs after the laser pulse is over, and which are emitted on a time scale very long compared to harmonic emission.[15]

After the single atom spectra have been calculated for a range of intensities of the driving field, they must be combined to obtain the coherent, macroscopic harmonic fields generated from the coherent emission of all of the atoms in the laser focus. This can be calculated by using the single atom polarization fields at the harmonic frequencies as source terms in Maxwell's equations. Solving the resulting equations allows a determination of the phase matching effects due to the different indices of refraction in the medium for the harmonic and driving fields, as well as the geometric phase introduced by the focusing of the laser. The phase matching contribution to the observed signal can be quite important, and it was not initially clear, based on traditional perturbation theory ideas, that high harmonic conversion efficiency in a single atom spectrum would imply a high conversion efficiency in the laboratory.[16,18]

Phase matching depends on the focal parameters of the laser, the gas density, the extent of ionization of the medium, and the active length of the medium. All of these effects have been included in a recent calculation of the phase matching effects in harmonic generation from xenon using the single atom spectra described above as the basic input. The agreement obtained with experiment was quite good.[15,17] Fig. 2. is a represenative result for the intensity dependence of the 15th harmonic. The main result of these calculations has been to realize the importance of the low order dependence of the harmonics on the laser intensity ($\sim I^5$) discussed above. In perturbation theory, where the harmonics scale as I^q, high order harmonic production is strongly concentrated in the center of the focal volume. In the strong field regime the harmonics vary much less rapidly with the driving laser intensity, leading to an increased volume for high order harmonic generation. This increase in volume reduces the rapid loss of coherence brought about by focusing and leads to almost constant phase matching factors for the harmonics in the plateau. Because of these effects, the existence of a plateau in the single atom spectrum leads in a straightforward way to a plateau in the experimental spectrum. The novel feature of this explanation for the formulation of the plateau is its dependence upon how the *amplitudes* of the harmonic fields vary rather than just their phases.[17]

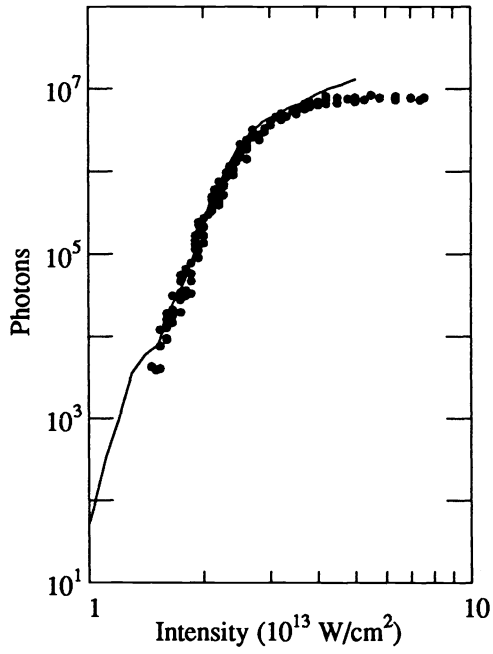

Fig. 2. Experiment (points) vs. Theory (line) for the 15th harmonic of 1064 nm in xenon.

PHOTON vs. ELECTRON EMISSION PROCESSES

Recently there has been considerable interest in the relationship between electron and photon emission, particularly with regard to the competition between processes of the same order. It has been proposed by several researchers that the emission of a photoelectron corresponding to the net adsorption of q laser photons should be closely related to the strength of the single atom emission of the qth harmonic photon.[19,20] This has been demonstrated to some degree with careful calculations for both processes over a range of intensities for both hydrogen and xenon.[21] The calculation of both electron and photon emission processes via the same formalism is a major advantage of time-dependent methods. In this section we present some results pertinent to the relationship between these processes in strong laser fields. The numerical methods used in obtaining the electron emission rates have been detailed elsewhere.

In Fig. 3, we show the emission rates of photons and electrons from xenon for a 1064 nm laser at five different peak intensities. The photo-emission rates are proportional to $q^3|d(q\omega)|^2$. Because there is an arbitrary multiplicative factor between the different rates, we have scaled the photon rate to agree with the electron emission rate at 3×10^{13} W/cm^2 for the 17th harmonic. This figure clearly shows the intensity dependence of processes of equal order are generally in quite good agreement. Only for the higher orders at the lowest two intensities is there an appreciable discrepancy between the photoelectron and harmonic emission spectra. This difference occurs because the production of a photon of frequency $q\omega$ requires not only the net absorption of q laser photons, but also the emission of the harmonic photon due to dipole coupling

between the excited state and the ground state. At low intensities, the dressed continuum states are poorly coupled to the ground state because the oscillator strength is concentrated within the bound state manifold. As the intensity increases, the dressed continuum states begin to include significant amplitudes of those bound state components which carry oscillator strength back to the ground state. Under these conditions the photoelectron and harmonic emission spectra become comparable. This agreement extends up to the point where the mixing between the bound and continuum states begins to decline. This point moves to higher and higher order with increasing intensity. These calculations provide dramatic evidence of the relationship between these processes. However, comparison between measured photon and electron rates must take into account the propagation of the harmonic fields through the excited volume, which may alter the apparent agreement which we have found between the single atom spectra.

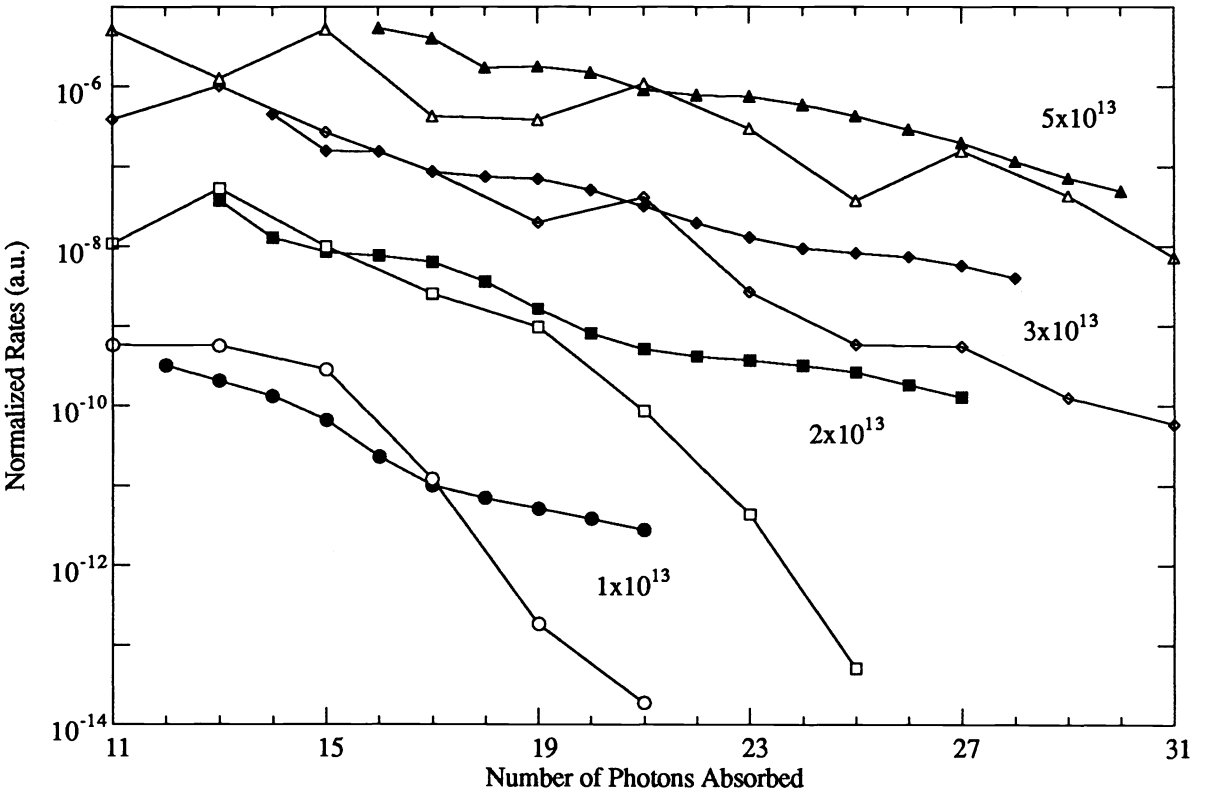

Fig. 3. Harmonic photon (open symbols) and electron (closed symbols) emission rates for xenon at 1064 nm as functions of intensity

SUMMARY

We have demonstrated the use of time-dependent methods in the calculation of high order optical harmonic generation from atoms in intense, pulsed laser fields. The treatment of the electron-ion and electron-laser interactions on an equal footings allows for the correct description the non-perturbative features of the problem. Future investigations will include harmonic generation from ions, higher peak laser intensities and the role of intermediate resonances in the enhancement of harmonic conversion.

This work was performed under the auspices of the U. S. Dept. of Energy at Lawrence Livermore National Laboratory under Contract No. W-7405-ENG-48. Partial support was provided to K.J.S. by National Science Foundation grant No. PHY87-11139.

REFERENCES

1. A. L'Huillier, L. Lompre, G. Mainfray, and C. Manus, "High order harmonic generation in rare gases," Adv. Atom. Mol. Opt. Phys. (1991) in press.

2. A. McPherson, G. Gibson, H. Jara, U. Johann, T. S. Luk, I. A. McIntyre, K. Boyer and C. K. Rhodes, "Studies of multiphoton of vacuum-ultraviolet radiation in the rare gases," J. Opt. Soc. Am. B **4**, (1987) 595-601; M. Ferray, A. L'Huillier, X. F. L.i, L. A. Lompré, G. Mainfray and C. Manus," Multiple-harmonic conversion of 1064 nm radiation in rare gases," J. Phys. B **21** (1988) L31-L35.

3. X. Li, A. L'Huillier, M. Ferray, L. A. Lompré and G. Mainfray, "Multiple-harmonic generation in rare gases at high laser intensity," Phys. Rev. A **39** (1989) 5751-5761.

4. S. J. Harris, private communication.

5. J. F. Reintjes, "Nonlinear Optical Parametric Processes in Liquids and Gases." Academic Press, Orlando, Florida (1984).

6. L. Pan, K.T. Taylor, and C. W. Clark, "Perturbation theory study of high harmonic generation," J. Opt. Soc. Am. B **7** (1990) 509-516.

7. R. M. Potvliege and R. Shakeshaft, "Multiphoton processes in an intense laser field: Harmonic generation and total ionization rates for atomic hydrogen," Phys. Rev. A **40** (1989) 3061-3079.

8. K. C. Kulander, K. J. Schafer, and J. L. Krause, "Time-dependent theory of multiphoton processes," Adv. Atom. Mol. Opt. Phys. (1991) in press.

9. K. C. Kulander, "Multiphoton ionization of hydrogen: A time-dependent theory," Phys. Rev. A **35** (1987) 445-447.

10. K. C. Kulander and T. N. Rescigno, "Effective Potentials for Time-Dependent Calculations of Multiphoton Processes in Atoms," Comp. Phys. Comm. **63** (1991) 523-528.

11. R Cowan, "Theory of Atomic Structure and Spectra," University of California Press, Berkeley, California (1981).

12. P. A. Christiansen, Y. S. Lee, K. S. Pitzer, "Improved *ab initio* effective core potentials for molecular calculations," J. Chem. Phys. **71** (1979) 4445-4450.

13. L. Kahn, P. Baybutt, and D. G. Truhlar, "*Ab initio* effective core potentials: Reduction of all-electron molecular structure calculations to calculations involving only valence electrons," J. Chem. Phys. **65** (1976) 3826-3853.

14. K. C. Kulander, "Time-dependent theory of multiphoton ionization of xenon," Phys. Rev. A **38** (1988) 778-787; K. C. Kulander and B. W. Shore, "Calculations of multiple-harmonic conversion of 1064-nm radiation in Xe," Phys. Rev. Lett. **62** (1989) 524-526.

15. A. L'Huillier, K. J. Schafer, and K. C. Kulander, "Theoretical aspects of intense field harmonic generation," J. Phys. B. (1991) in press.

16. B. W. Shore and K. C. Kulander, "Generation of optical harmonics by intense pulses of laser radiation I. Propagation effects," J. Mod. Opt. **36** (1989) 857-875; K. C. Kulander and B. W. Shore, "Generation of optical harmonics by intense pulses of laser radiation II. Single atom spectrum for Xe," J. Opt. Soc. Am. B **7** (1990) 502-508.

17. A. L'Huillier, K. J. Schafer, and K. C. Kulander, "High order harmonic generation in xenon at 1064 nm: The role of phase matching," Phys. Rev. Lett. 66, 2200 (1991).

18. A. L'Huillier, L. Lompre, G. Mainfray, and C. Manus, "High order harmonic generation in rare gases," Adv. Atom. Mol. Opt. Phys. (1991) in press.

19 B. W. Shore and P. L. Knight, "Enhancement of high optical harmonics by excessphoton ionization," J. Phys. B 20, 413 – 423 (1987).

20. J. H. Eberly, Q. Su and J. Javanainen, "Nonlinear light scattering accompanying multiphoton ionization," Phys. Rev. Lett. 62, 881 – 884 (1989).

21. K. J. Schafer, J. L. Krause and K. C. Kulander, "Nonlinear effects in electron and photon emission from atoms in intense laser fields," J. Nonlin. Opt., in press.